

# Methods of Evaluating and Mitigating NVH when Operating an Engine in Dynamic Skip Fire

Joe Serrano, Geoff Routledge, Norman Lo, Mark Shost, Vijay Srinivasan,  
 and Biswa Ghosh  
 Tula Technology

## ABSTRACT

Cylinder deactivation is a technology seeing increased automotive deployment in light of more demanding fuel economy and emissions requirements. Examples of current production systems include GM's Active Fuel Management and Chrysler's Multi-Displacement System, both of which provide one fixed level of deactivation. Dynamic Skip Fire (DSF), in which the number of fired cylinders is continuously varied to match the torque demand, offers significantly increased fuel savings over a wider operating range than the current production systems. One of the biggest challenges in implementing cylinder deactivation is developing strategies to provide acceptable Noise, Vibration and Harshness (NVH); this paper discusses those challenges and the methodologies developed. This work covers theoretical root causes; proposed metrics to quantify the NVH level; algorithmic and physical mitigation methods; and both subjective and objective evaluation results.

**CITATION:** Serrano, J., Routledge, G., Lo, N., Shost, M. et al., "Methods of Evaluating and Mitigating NVH when Operating an Engine in Dynamic Skip Fire," *SAE Int. J. Engines* 7(3):2014, doi:10.4271/2014-01-1675.

## INTRODUCTION

Cylinder deactivation technology has been demonstrated as a durable and reliable means to achieve improved fuel economy in spark ignited gasoline engines. Notable current production systems include GM's Active Fuel Management (AFM) [2] and Chrysler's Multi-Displacement System (MDS) [3], both deployed on production V8 engines. Recently increased Corporate Average Fuel Economy standards in the US and CO<sub>2</sub> targets in Europe have driven application of cylinder deactivation to smaller displacement and lower cylinder count engines. This can be seen with Volkswagen's application of Active Cylinder Technology (ACT) in its new 1.4L turbo GDi engine in 2013.

Cylinder deactivation achieves fuel economy improvement by operating a reduced number of cylinders at a higher operating load per cylinder to produce the same engine torque output. These systems are examples of two-mode deactivation where either full cylinder count or half cylinder count is provided, V8 or V4 mode and L4 or L2 mode as shown in Figure 1. Such systems are even firing, which means a skipped cylinder event follows a firing cylinder and the firing sequence or pattern is completed with each engine cycle.

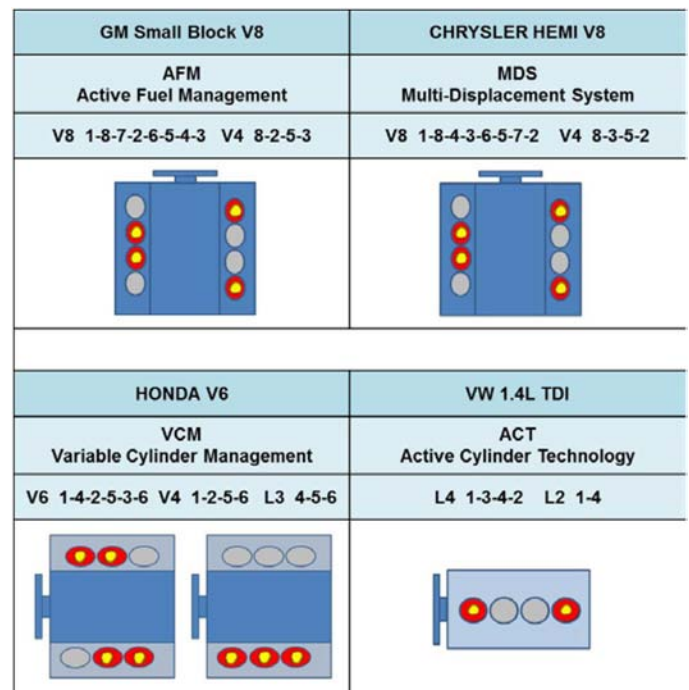


Figure 1. Cylinder deactivation systems as deployed by GM, Chrysler, Honda and VW

Automakers have also implemented cylinder deactivation systems that result in uneven firing. Honda introduced a V4 mode to its V6/L3 deactivation engine [4, 5]. GM recently introduced a V4 mode to its fifth generation small block based V6 engine family for 2014 model year. These systems are also shown in Figure 1. They provide two cylinder firing events followed by a skipped cylinder event. Similar to the 2-mode applications these systems complete the firing sequence or pattern with each engine cycle.

An alternative approach is to consider firing sequences that require more than one engine cycle to complete their sequence or pattern. This idea is not new; the first example is described US patent 2771867 [6], which describes a method for running a four cylinder engine at multiples of 1/9 of full power. US patent 4509488 [7] extends this idea to many fractions of full power. If we extend this paradigm to any possible firing sequence with even or uneven firing we have DSF operation where the engine is continuously operated at high thermal efficiency. DSF incorporates any-time, any-cylinder deactivation and can continuously vary the number of cylinders firing, along with cylinder load to provide for flexible control of acoustic and vibrational excitations from the engine. The fuel economy benefits of DSF are shown to be 14-17% composite fuel economy improvement over standard V8 operation [1].

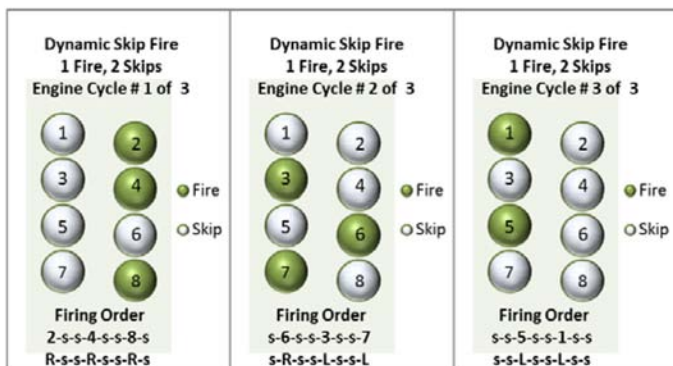


Figure 2. An example of a firing sequence that fires one cylinder followed by two skipped cylinders. The pattern will repeat after three engine cycles for an 8 cylinder engine.

In this paper we will investigate one particular sequence of interest, a cylinder firing followed by two cylinder skips. If applied to an engine of eight cylinders the patterns will repeat after three engine cycles. If we start the sequence on cylinder #2, then using the GM small block firing order from Figure 1 we have three firing cylinders in the first engine cycle, followed by three firing cylinders in the second engine cycle and two firing cylinders in the third engine cycle as shown in Figure 2. Although the number of fired cylinders per engine cycle varies for our eight cylinder engine, the sequence itself is defined as even firing with each firing followed by two skips. Another characteristic of this sequence is that all the cylinders will be fired in the three engine cycles providing a rotating pattern to distribute thermal load and avoid any prolonged cylinder deactivation that can result in spark plug fouling. It should be noted that the sequence is not limited to start on cylinder #2 but can be entered on any cylinder number and followed for

three engine cycles where it will repeat. Of course this is not the only sequence to fire eight cylinders in three engine cycles. In fact there are 735,471 sequences that fire eight times and skip 16 times in three engine cycles. The challenge, then, is to select the patterns with acceptable NVH.

## 1. VIBRATION

One of the primary challenges of using DSF is the resulting increase in the level of vibration that running the engine in a skip fire mode induces in the vehicle. One straightforward source is the fore-aft vibration on the entire vehicle induced by the changing levels of vehicle acceleration.

Each time a cylinder fires, the torque generated accelerates the vehicle, causing an excitation that may be felt by the vehicle occupants. At 1500 engine RPM a four-stroke V8 will fire 100 times per second. If we were to assume that all of the torque pulses generated by the cylinders were identical, then the lowest fore-aft acceleration frequency would be 100 Hz. However, when running in DSF, the frequencies of vibration will be quite different. For a given pattern, though, the spectrum of the fore-aft acceleration can be approximately determined. Continuing the example from before, if the skip/fire pattern is one fire followed by two skips (*fire-skip-skip*), then the lowest fore-aft acceleration frequency will be 33.33 Hz, since the pattern repeats every 30 ms. The time domain waveform of the flywheel torsional speed that arises from such a pattern is shown in Figure 3. Its frequency spectrum is shown in Figure 4. (The constant portion of the waveform has been removed.)

This very simple model is informative and tells us that the fundamental frequency of this pattern is high enough that it should be quite acceptable (see Section 3). However, two things can occur that make it less ideal. First, if a resonance at about 33 Hz exists in the powertrain or between the powertrain and driver, the magnitude of the vibration can be significantly increased. In this case this pattern may be unsuitable at this RPM. Second, if the resonance occurs instead at, say, 25 Hz, then the pattern may be unacceptable when the RPM is 1100-1150. Thus the quality of the various patterns can change markedly as the engine speed changes.

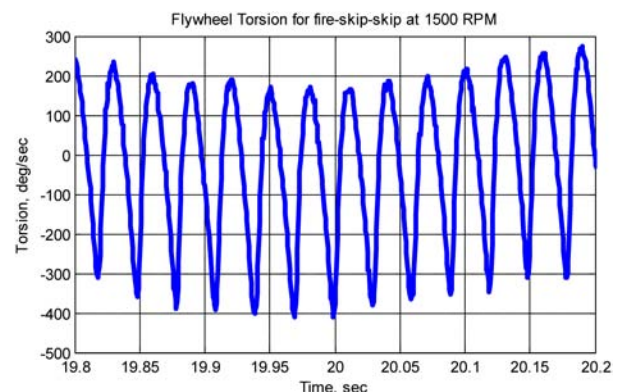


Figure 3. Flywheel torsion versus time for a fire-skip-skip pattern, DC term removed

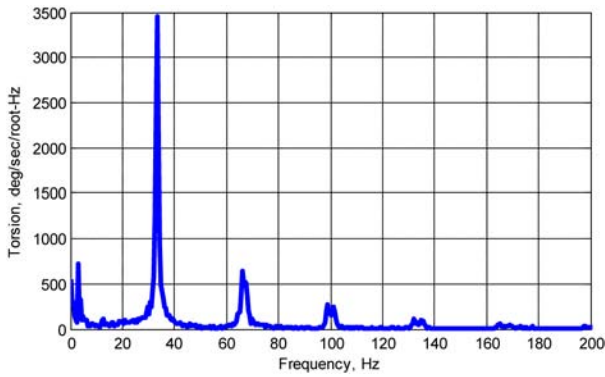


Figure 4. Flywheel Torsion versus frequency for a fire-skip-skip pattern

The way in which the powertrain excitation enters the cabin as low frequency vibration depends upon the many transfer path sensitivities as well as the primary rigid body modes of the body and the powertrain. For an SUV with a body-on-frame there can be significant low frequency modes (as shown on Figure 5) that have to be managed to minimize excitation. Human vibration sensitivity tends to occur between 1 to 18 Hz with peak sensitivity being around 4 Hz

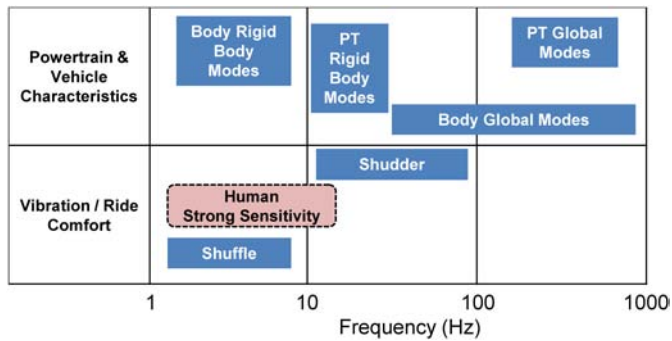


Figure 5. Comparison of vehicle modal characteristics and highest vibration sensitivity for humans

With DSF it is therefore important to optimize the excitation and the transfer paths in order to minimize vibration into the vehicle.

While the frequency of the torsional vibration depends on the pattern being used, the peak-to-peak variation depends on the firing density. Figure 6 shows the change in velocity of engine speed for different firing densities. As can be observed, the velocity amplitude decreases as the firing density increases.

In terms of human sensitivity to these speed fluctuations it was found that only the 20% firing density was considered unacceptable at this speed & load. So while care has to be taken in the calibration of the DSF system to ensure that N&V and comfort targets are met, the task is not insurmountable.

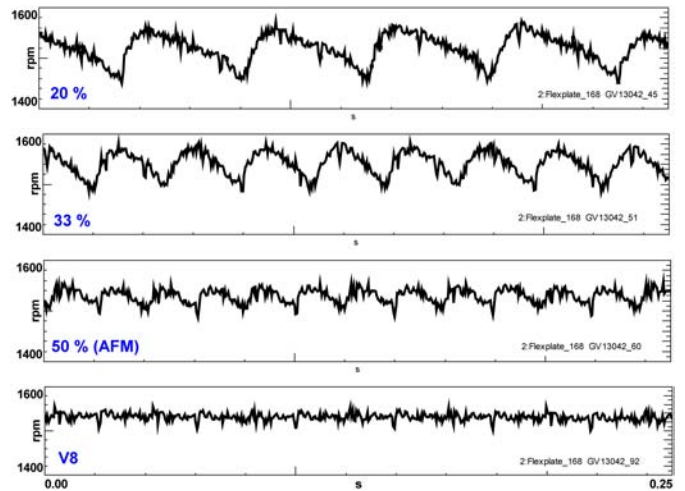


Figure 6. Comparison of engine speed velocity during constant speed (1500rpm, 3rd gear, same TCC slip) for various firing densities

## 2. ACOUSTICS

Each skip/fire pattern creates not only a signature vibration, but also a signature acoustic pattern. However, the basic model to describe the acoustic effect is more complicated than was the case for fore-aft vibration. With vibration, a simplifying assumption is that each torque pulse from firing a cylinder is identical. For acoustics, we assume that the sound of each firing is the same, except that each cylinder has a different length path from the exhaust valve to the tailpipe outlet. As a result, the position of each pressure pulse is modulated over time, potentially introducing additional frequencies. This can be illustrated with a simple model that assumes that 1) the *fire-skip-skip* pattern discussed is used, 2) the RPM is 1500, and 3) the path length for odd cylinders is longer than for even cylinders because of an uneven Y-pipe length. Such a Y-pipe is often found in production applications.

Figure 7 shows a time plot of a simulation of a series of sound pressure pulses from a cylinder firing sequence. The green line shows the case that the Y-pipe is equal length, while the blue line shows the case when the Y-pipe has a difference of about 1 meter between legs. This path length difference shows up when four consecutive firings are delayed relative to the other four. If, as occurs in a V8 engine like the GM small block from Figure 1 with firing order 1-8-7-2-6-5-4-3, then with this pattern for *fire-skip-skip*, the firing sequence starting on cylinder 2 is 2-s-s-4-s-s-8-s-s-6-s-s-3-s-s-7-s-s-5-s-s-1. (Each fire is given by the cylinder number and is separated by two skips.) So this pattern fires four times on one bank (even cylinder numbers) and then four times on the other bank (the odd cylinder numbers.) See Figure 2 for illustration where the two lines overlap for the firings on one bank but are offset for the firings on the other bank.

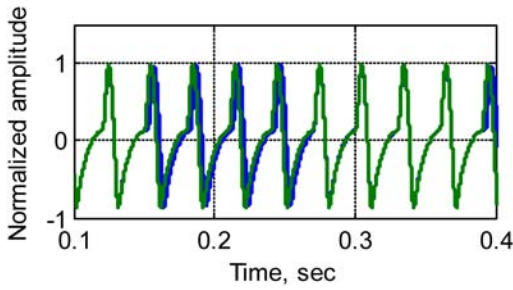


Figure 7. Sound pressure versus time for equal-length Y-pipe versus one with unequal length at tailpipe outlet

The following figure (Figure 8) shows the two frequency responses for the two time waveforms in Figure 7. The green line corresponds to the equal length Y-pipe, and has frequency content only at 33 1/3 Hz and its harmonics. The blue line, on the other hand, corresponds to the unequal Y-pipe. It has additional spurs from the equal length case, displaced from the main spurs by 4 1/6 Hz, the rate of modulation of the pulses' position.

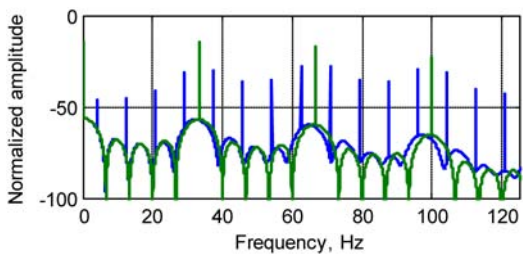


Figure 8. Sound spectra for the waveforms of Figure 7

These additional spurs act to cause an audible change at a frequency of 4 1/6 Hz, or 1/8 of 33 1/3 Hz. Psycho-acoustic effects of this firing pattern will be discussed more in section 3.3 where the concept of fluctuation is discussed. But one additional thing to notice here is that the extra spurs increase in magnitude relative to the center spurs (the 33 1/3 Hz harmonics) with increasing frequency. This is a mathematical consequence of the modulation of the pulse position, and manifests itself as more noticeable modulation with increasing frequency. Thus the amount of modulation grows precisely in a frequency band to which the ear is more sensitive.

### 3. METRICS FOR VIBRATION AND ACOUSTICS

#### 3.1. Measuring Comfort

This section describes two techniques for evaluating ride comfort: ISO-2631 [8] and the Sperling Index [9,10,11,12]. ISO-2631 provides a standard model for evaluating human exposure to whole-body vibration. The basic measure is the weighted root-mean-square (RMS) acceleration as given by

$$a_w = \sqrt{\frac{1}{N} \cdot \sum_{n=0}^{N-1} a_w(n)^2}$$

where  $a_w(n)$  is the weighted acceleration as a function of samples and  $N$  is the number of samples in the measurement. The weighting of the acceleration is given by one of a set of comfort weighting functions ( $W_c$ ,  $W_d$ ,  $W_e$ ,  $W_f$ ,  $W_k$ , and  $W_j$ ) specified in the frequency domain for different applications and can be decomposed into component transfer functions. Refer to [8] for the transfer functions and parameter definitions. For evaluating comfort,  $W_d$  is used for weighting the horizontal directions and  $W_k$  is used for weighting the vertical direction.

Sperling's method, also known as the  $W_z$  (Wertzungzahl) method, was initially proposed to measure ride comfort in locomotives [10, 12]. The Sperling index can be implemented using the discrete Fourier transform (DFT) with the following calculation [9]

$$W_z = \sqrt[10]{\sum_{i=0}^{N_f} [2 \cdot a_i \cdot B(f_i)]^3}$$

where  $a_i$  is the magnitude of the  $i^{\text{th}}$  frequency index (from the acceleration DFT) in  $m/s^2$ ,  $N_f$  is the spectrum of acceleration response, and  $B(f)$  is the Sperling weighting curve given by

$$B(f) = k \cdot \sqrt{\frac{1.911f^2 + (0.25f^2)^2}{(1 - 0.277f^2)^2 + (1.563f - 0.0368f^3)^2}}$$

where  $k = 0.737$  for horizontal and  $0.588$  for vertical direction.

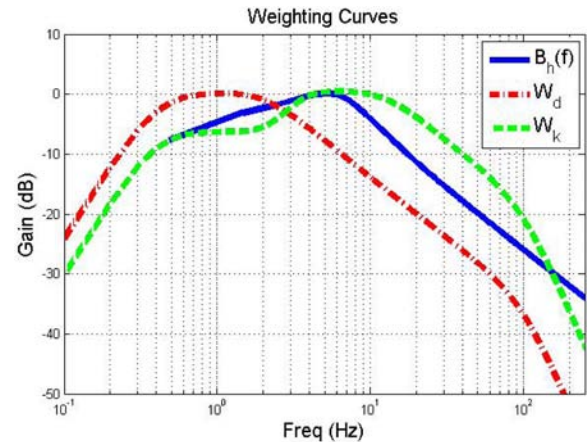


Figure 9. Comfort weighting curves:  $W_d$ ,  $W_k$ , and  $B$  (Sperling)

The frequency weighting curves for the ISO-2631 and Sperling comfort metrics are shown in Figure 9. The  $W_d$  curve is used to scale fore-aft and lateral vibration, and has a lower frequency response (bandwidth from ~0.4 - 2.8 Hz) while  $W_k$  is used for scaling vertical vibration (bandwidth from ~2.8-18 Hz). The bandwidth of the Sperling weighting curve is between  $W_d$  and  $W_k$  (from 1.5-9 Hz). For both metrics, human sensitivity to comfort is weighted more heavily at low frequencies.

The Sperling index maps to a subjective evaluation of ride comfort in the range of 1 to 4 given in Table 1.

Table 1. Sperling index

W <sub>z</sub>	Ride Comfort
1	Just noticeable
2	Clearly noticeable
2.5	More pronounced but not unpleasant
3	Strong, irregular but still tolerable
3.25	Very irregular
3.5	Extremely irregular, unpleasant, annoying; prolonged exposure intolerable
4	Extremely unpleasant; prolonged exposure harmful

### 3.2. Objective/Subjective Correlation

To facilitate calibration of the DSF system, it was deemed desirable to have an objectively measured metric for ride comfort that corresponds to the vehicle occupant's subjective sense of comfort. This section describes the mapping of the Sperling index from Table 1 to automotive applications. Table 2 shows a typical subjective scoring for vibration and comfort in the automotive industry. This is the scoring system used at Tula Technology.

Table 2. Typical subjective rating scale used for N&V evaluation

UNACCEPTABLE				
1	2	3	4	5
Dangerous To Health Safety Risk	Frightening	Bad Intolerable & must be corrected	Poor Very Annoying	Borderline Borders on Being Annoying
ACCEPTABLE				
6	7	8	9	10
Acceptable Generally noticed but considered tolerable by the customer	Good Noticed only by perceptive customers Not considered a problem	Very Good Not observed by customers Observed by Trained personnel only	Exceptional Not Observed by customers Barely Perceived by trained personnel	Perfect No issue observed

#### 3.2.1. Test Environment

A controlled environment is paramount to the consistency and validity of the experiments. Therefore, tests were conducted on a vehicle dynamometer, where the test environment is controllable and reproducible. The vehicle operated with the following target conditions: 1500 RPM, 80 kPa MAP, cam retard angle of 40°, and target torque converter clutch (TCC) slip of 60 RPM. Vibration spectra were stimulated using different excitation patterns (skip/fire patterns). Seat rail accelerometer data was collected using the LMS SCADAS system running Test-Lab software.

#### 3.2.2. Testing Methodology

To ensure repeatability in the experiments, the following guidelines were adhered to in developing tests:

1. A jury of four evaluators was selected to score the subjective experience using the scale shown in Table 2.
2. Before data collection, initial "human calibration" tests were performed to establish a reference base line. A range of operating conditions (from pleasant to harsh) was used to provide a complete range of experience.
3. During data collection, the evaluations were performed "blind," where evaluators are unaware of test conditions and cannot communicate with each other.
4. Tests were grouped together based on the following properties:
  - a. Tests with similar expected response were grouped together to help establish a subjective sensitivity threshold.
  - b. Tests with very different expected response were also grouped together to allow evaluators to experience the range of conditions and remove memory effects.
  - c. The final group of tests contained conditions that were considered a mixture of good and bad.
  - d. Reference tests for both pleasant and harsh conditions were interspersed between test groups. This was done to help recalibrate the evaluator's subjective scoring as well as verify scoring consistency.

To establish individual evaluator's sensitivity, the same tests were repeated on different days with the evaluators reprising the same seat location. The test order was rearranged but maintained the same properties outlined in item 4.

#### 3.2.3. Testing Results

Figure 10 shows good correlation between subjective scores and the calculated Sperling index from data collected over three days of vehicle dynamometer testing.

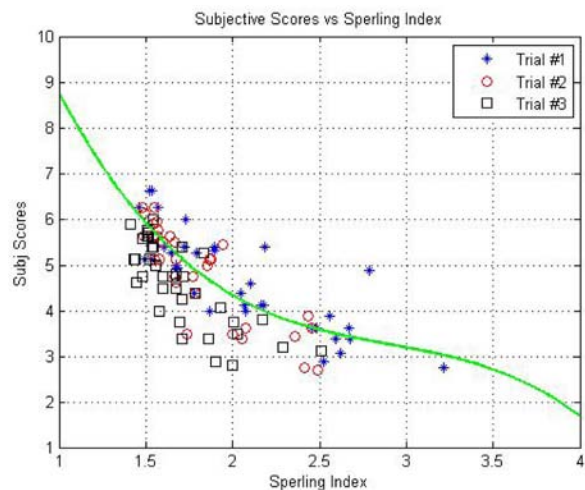


Figure 10. Mapping from Sperling index to an automotive subjective score

The relationship between the subjective and Sperling index can be established using polynomial regression as shown by the green curve.

Figure 11 shows the variability of evaluators' scores against measured Sperling scores over common operating conditions. Given the same testing conditions, subjective human scores can vary significantly compared to a measured score.

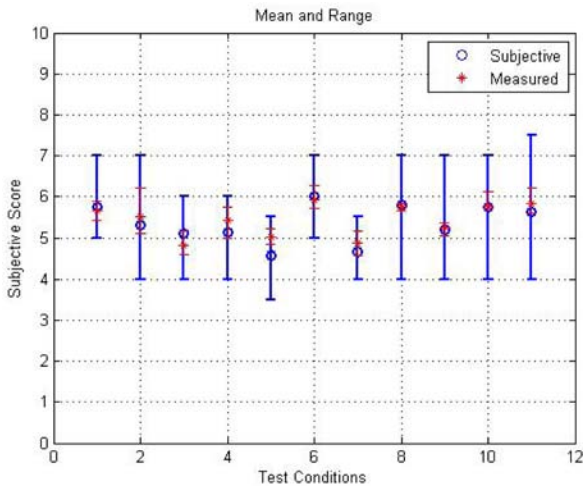


Figure 11. Variability between subjective scores and calculated subjective score

### 3.3. Acoustic Metric

Quantifying sound quality involves modeling psychoacoustic response. Loudness, the perception of intensity, is one of the most commonly used metrics and is described by different standards (ISO 532 A/B, 226:2003; ANSI S3.4-2997, and DIN 45631). Unfortunately, other metrics that model different acoustic phenomena are less developed. These metrics include sharpness, roughness, fluctuation strength, pitch, tonality, articulation index, and prominence ratio [13]. Of these, fluctuation plays an important role as described in section 2.

Finite length firing patterns repeat and can be characterized by their spectral response. Some of these patterns interact with the physical structure of the engine to cause acoustic effects. For some firing patterns, physical structures such as unequal exhaust pipes can impose a modulating effect on the underlying acoustic response. A technique to quantify the impact of these effects is to measure the modulation index of the acoustic waveform. This section describes modulation phenomena and presents a technique to calculate it.

#### 3.3.1. Measuring Modulation

Modulation describes the interaction of multiple tones in a signal. The perception of the sound depends on the modulation depth (strength), modulation frequency, and center (or carrier) frequency. Figure 12 shows modulation frequency  $f_{mod}$  and modulation depth  $\Delta L$ .

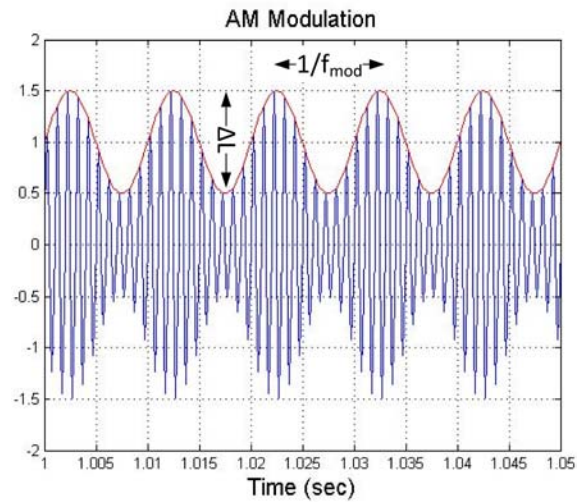


Figure 12. Describing modulation with modulation depth and modulation frequency

A signal with modulation frequency higher than 20 Hz is generally perceived as sounding "rough". Roughness can be characterized as [13]

$$R \approx f_{mod} \cdot \Delta L$$

and is measured in units of asper (Latin for rough). One asper is defined as 1 kHz tone at 60 dB with 100% amplitude modulation at 70 Hz. At a modulation frequency of 20 Hz, the rough modulating sound transitions to a fluctuation sound. Fluctuation strength can be calculated as [13]

$$F \approx \frac{\Delta L}{\frac{f_{mod}}{4} + \frac{4}{f_{mod}}} = \alpha_{mod} \cdot \Delta L$$

Fluctuation strength is measured in units of vacil (Latin). One vacil is defined to be a 60 dB tone at 1 kHz with 100% amplitude modulation at 4 Hz.

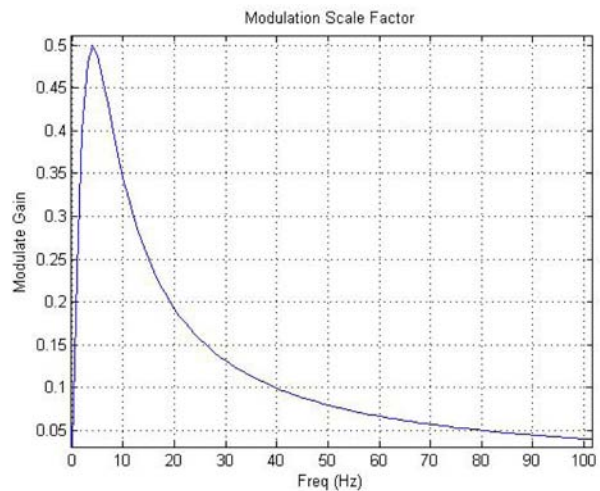


Figure 13. Psycho-acoustic weighting of modulation

Figure 13 shows the modulation weighting coefficient as a function of frequency where fluctuation strength is strongest at 4 Hz.

### 3.3.2. Algorithm Description

The algorithm described here estimates the modulation parameters at sub-bands defined by the harmonics in the firing pattern's spectrum. The envelope spectrum of each sub-band is used to estimate the modulation depth and frequencies. Modulation weighting (as shown in Figure 13) and loudness weighting (such as A-weighting) are applied to model psychoacoustic phenomena.

To model human hearing response, loudness weighting is applied. The signal is then decomposed into sub-bands defined by the firing patterns' harmonics. The sub-band envelope is calculated using the Hilbert transform to construct an analytic signal. The signal is demodulated and filtered to extract the bandwidth of interest.

The analytic signal calculation is calculated as

$$y_A(n) = y(n) + j \cdot \hat{y}(n)$$

where  $\hat{y}(n)$  is the Hilbert transform of  $y(n)$ , and the Hilbert transform is defined as

$$H_{HT}(f) = \begin{cases} -j & f \geq 0 \\ j & f < 0 \end{cases}$$

The baseband signal can be calculated by demodulating harmonics of the firing pattern's fundamental frequency

$$y_{B^k}(n) = y_A(n) \cdot e^{-j\frac{2\pi k F_0 n}{F_s}}$$

$k$  - sub-band index

$F_0$  - fundamental frequency of firing pattern

$F_s$  - sampling frequency

The baseband equivalent of the sub-band signal is extracted by low pass filtering the demodulated signal as expressed below and depicted in Figure 14.

$$\hat{Y}_{B^k}(f) = \begin{cases} Y_{B^k}(f) & -\frac{F_0}{2} < f < \frac{F_0}{2} \\ 0 & \text{otherwise} \end{cases}$$

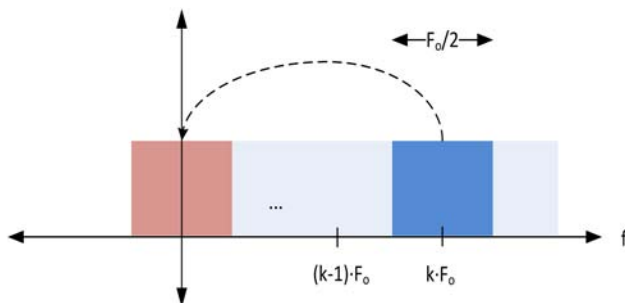


Figure 14. Baseband equivalent of sub-band

For each sub-band (and dropping index  $k$  to simplify notation), the envelope is calculated as

$$y_{env}(n) = \sqrt{|Real(\hat{y}_B(n))|^2 + |Imag(\hat{y}_B(n))|^2}$$

Modulation depth and frequencies are estimated from the spectrum of the envelope signal. Figure 15 illustrates the concept of the algorithm. An intensity weighting is applied to the signal to model loudness (top black curve). A sub-band based on the harmonics of the firing pattern is extracted (top red curve). The sub-band envelope is calculated (second blue curve). The spectrum of the envelope is then calculated to estimate power and frequency of the modulation tones (bottom blue curve). To model psychoacoustic effects, modulation weighting is applied to the modulation tones. For each sub-band, the modulation index is scaled by the sub-band power.

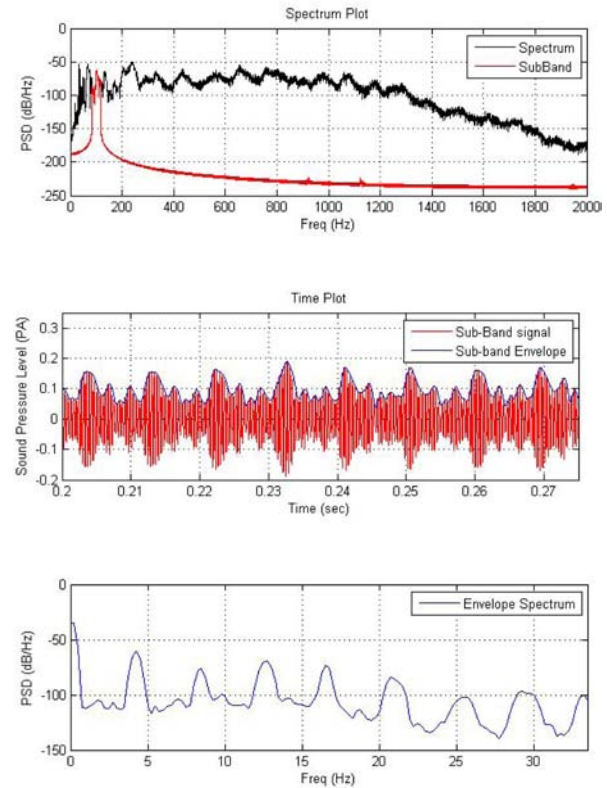


Figure 15. Illustration of modulation metric calculation

In this development, modulation depth is calculated as the ratio between the power of the modulation and carrier frequency. The modulation frequency is the difference between the sub-band carrier and the modulation tone. The overall sub-band modulation tone power is calculated as the weighted power of all modulation tones. More formally, the sub-band modulation index can be described as

$$\Delta l_i = \frac{2 \sum_{j=1}^M \alpha_j^2 P_j}{P_{c,i}}$$

$\Delta I_i$  - modulation index for  $i^{\text{th}}$  sub-band

$i$  - index to sub-band as defined by the firing pattern's spectrum

$j$  - index of modulation tone

$M$  - number of modulation tones

$\alpha_j$  - modulation factor as shown in [Figure 13](#)

$P_j$  - modulation tone power (single-side band)

$P_{c,i}$  - harmonic tone power (on  $i^{\text{th}}$  tone)

The overall modulation metric value can then be calculated as the loudness weighted sum of all the sub-band modulation indices.

$$m = \sum_{i=0}^N \Delta I_i \cdot \chi_i$$

$i$  - sub-band index,  $N$  - total number of sub-bands

$\Delta I_i$  - modulation index for  $i^{\text{th}}$  sub-band

$\chi_i$  - power density in  $i^{\text{th}}$  sub-band (a-weighted spectrum)

Spectral weighting of sub-band power reflects the psychoacoustic response to signal intensity at each of the sub-bands. For the development of this algorithm, A-weighting [14] was performed and other weighting (B, C, D) can be performed depending on applications.

### 3.3.3. Results

[Table 3](#) shows the modulation metric used to measure the all-cylinder firing and the 1-in-3 (*fire-skip-skip*) cylinder-firing scenarios with both the exhaust control valve (ECV) engaged and disengaged. (The ECV is discussed in [section 5.2.3](#).) The data was collected with the vehicle operating at a reference RPM, and only the firing pattern was varied. The modulation metrics presented here are expressed as a percentage. The scores are further normalized over the total signal power. This allows for comparison of modulation in data captures with different over-all intensities. The metric above is then calculated as

$$m = \frac{1}{S_T} \sum_{i=0}^N \Delta I_i \cdot S_i$$

$\Delta I_i$  - modulation index for  $i^{\text{th}}$  sub-band

$S_i$  - power in  $i^{\text{th}}$  sub-band

$S_T = \sum_{i=0}^N S_i$  - total power over all sub-bands

With the ECV disengaged, the results shows that the 1-in-3 cylinder firing scenario has a higher modulation score than when all the cylinders are firing. When the ECV is engaged, both metric scores are improved (the modulation metric is lowered). The all-cylinder firing scenario scores better than the 1-in-3 cylinder firing scenario.

Table 3. modulation metric scores

Description	Modulation Metric (%)
ECV OFF all cylinder firing	2.21
ECV OFF 1-in-3 cylinder firing	9.25
ECV ON all cylinder firing	0.25
ECV ON 1-in-3 cylinder firing	5.25

## 4. ALGORITHMIC MITIGATION

As the examples in [section 2](#) and [section 3](#) showed, fixed patterns can cause both vibrational and acoustic issues. A particular pattern can be fine at one RPM, but have unpleasant vibration at another. Or a particular pattern can cause acceptable vibration but generate an unpleasant sound. Careful selection of the firing sequence can mitigate these problems.

For one example, at 1500 RPM the pattern *fire-skip-skip* discussed above has the advantage that it concentrates the vibration energy at the relatively high frequency of 33 Hz, which lies outside the band of human sensitivity. But let us suppose that there is a resonance in the driveline at 33 Hz. The advantage of having all the energy at relatively high frequency is now a disadvantage, as this effect can create excessive fore-aft vibration due to the resonance. In this event, there are a number of ways to mitigate the problem. A straightforward solution is to use a different pattern with the same proportion of fires to skips. A candidate pattern might be *fire-skip-skip-skip-fire-skip*. Since this pattern is twice as long the original, the fundamental frequency of the new pattern will be half that of the original pattern. Its second harmonic will still lie on the resonance (having the same frequency as the original patterns fundamental) but will have a magnitude half the original pattern. Thus this new pattern may prove itself to be superior, at least over a narrow engine speed range.

A second method to address this problem is to use a pattern with a different ratio of fires to skips. For example, a ratio of two fires to three skips will produce approximately the same amount of torque. The difference can be compensated by changing other engine parameters, for example by throttling the engine slightly more to offset the increased proportion of firing. Now, the pattern length is five firing opportunities long (*fire-skip-skip-fire-skip*), so at 1500 RPM, the fundamental frequency of the pattern will be 20 Hz. While the fundamental is lower than for the original pattern, both it and its second harmonic fall well away from the resonance at 33 Hz. [Figure 16](#) shows the spectra of the translational vibration for these patterns.

Longer patterns can also be considered. For example, a pattern of seven fires and thirteen skips will have a fundamental frequency of 5 Hz, with harmonics at 30 and 35 Hz.

However, while the harmonics may be adequately small and far enough from the resonance so as not to create a problem, as discussed in the metric section the low frequency fundamental can cause an unpleasantly perceptible amount of vibration.

Indeed, all patterns have a fundamental frequency for a given RPM. As the RPM changes, the perceived vibration changes. Thus one way to mitigate vibration is simply to find a qualifying RPM for each pattern, and refuse to use that pattern when the engine speed is outside this range. Unfortunately, such a simple qualification scheme, while useful against vibrations, is not useful to mitigate acoustics. The modulation frequency of the *fire-skip-skip* pattern is 4 Hz at 1440 RPM. For any engine speed from 500 to 3000, the frequency of fluctuation will still be within an annoying range. Since the amplitude of the acoustic signature decreases with cylinder charge, we could restrict ourselves to using this pattern at low loads. However, because one goal of DSF is to keep the load on each cylinder relatively high, this should not be a frequent occurrence. We instead must completely stop using the pattern, or find non-algorithmic ways to mitigate the acoustics. Not using the pattern requires no added cost, but will impact overall fuel efficiency.

Figure 17 shows the acoustic spectra of the patterns from Figure 16.

The software mitigation can also be used as a powerful tool to avoid powertrain and vehicle related resonance modes. With conventional engines the firing frequency increases as the engine speed increases and at some point there will be an engine or vehicle resonance that will be excited by this. Normal mitigation methods (physical hardware) are used in this instance to minimize the resonance so that the vehicle passengers experience acceptable NVH.

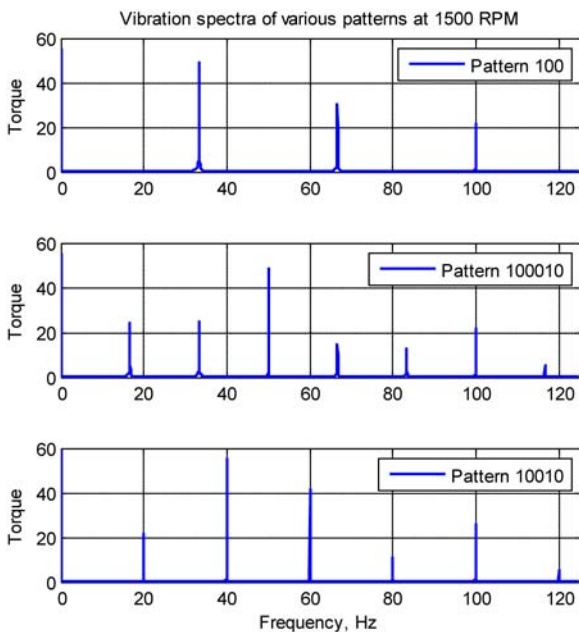


Figure 16. Vibration spectra for various patterns

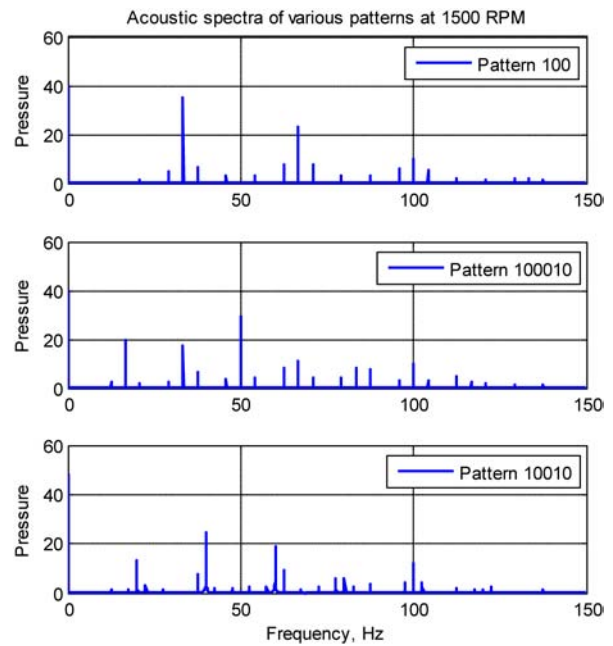


Figure 17. Acoustic spectra for various patterns

With DSF it is possible to avoid exciting the resonance modes by selecting the firing pattern / sequence at each RPM to avoid patterns which have spectral content at the resonance frequency. This opens up potential opportunities to reduce the amount of NVH enablers required and thereby reducing weight and cost.

An example is given in Figure 18 where a significant low frequency boom at 46 Hz was eliminated using a resonance avoidance method in the software.

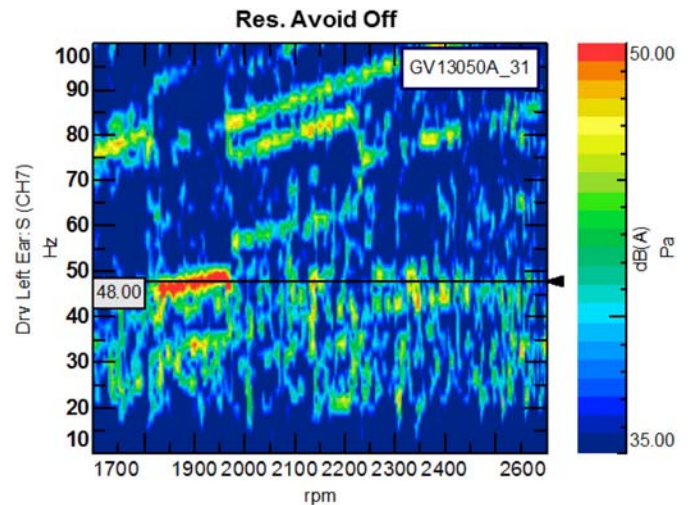


Figure 18. Elimination of 46 Hz Boom using software mitigation

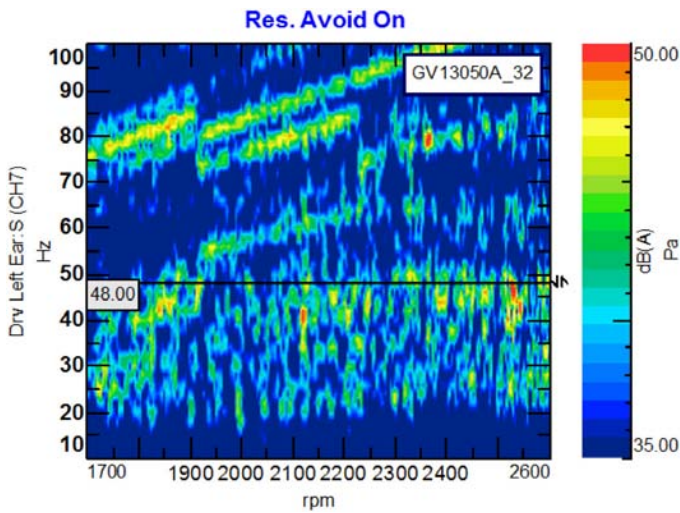


Figure 18. (cont.) Elimination of 46 Hz Boom using software mitigation

## 5. PHYSICAL MITIGATION

To complement the software NVH refinement, additional development work was performed to find the most efficient NVH enablers. The work was performed on a production 2010 GMC Yukon Denali fitted with a V8 engine modified to run DSF [1].

### 5.1. Acoustic Mitigation

Initial Tula development focused on physical acoustic mitigation for two reasons. One is that acoustic modulation was the dominate NVH concern for DSF operation. The second is that algorithmic solutions carried an undesirable fuel efficiency cost.

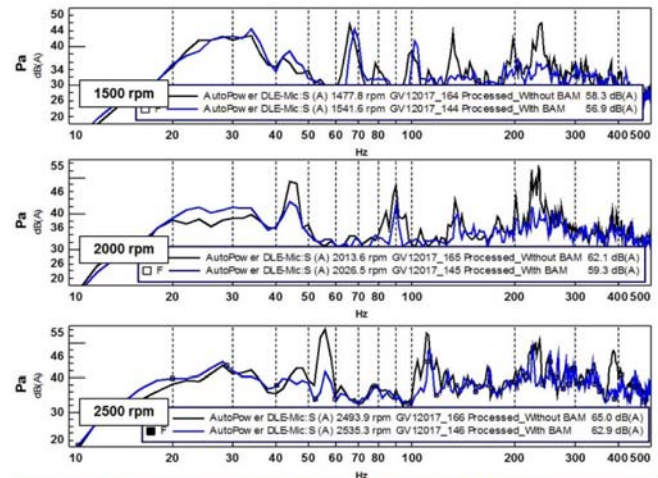
#### 5.1.1. Intake & Exhaust Orifice Noise

Subjectively, it was perceived that interior noise was dominated by the exhaust orifice radiated noise rather than structure-borne noise. To confirm the contribution of the intake and exhaust orifice noise to the interior noise, Big Auxiliary Mufflers (BAM) were used to effectively eliminate the orifice noise for each. The effect of the intake and exhaust BAM are shown below (subjective + objective) in Figure 19 and Figure 20. The four seat ratings are shown individually for each condition

It can be observed that subjectively the Exhaust BAM showed the biggest influence on the interior noise, the intake BAM actually showing an overall detrimental effect, due to an increased high frequency noise with the intake BAM in place.

BAM Config	Ratings relative to 'No BAM' Config									
	2nd Gear Full Pedal	3rd Gear Part Pedal Accel	2nd G Steady 1500rpm	3rd G Steady 1500rpm	4th G Steady 1500rpm	2nd G Steady 1500rpm	3rd G Steady 1500rpm	4th G Steady 1500rpm	2nd G Steady 1500rpm	3rd G Steady 1500rpm
No BAM	0	0	0	0	0	0	0	0	0	0
Intake BAM	0	-0.5	0	0	-0.33	-0.67	-1	-0.34	-0.17	-0.33
Exhaust BAM	0	-0.17	0	0	1.34	0.67	1.08	1.08	1	1.17
Both BAMs	0	1	0	0	-0.33	-0.17	0.4967	0.33	0.5	0.84
	0	0.33	0.33	0	1.17	1	1.33	0.5	1.16	1.17

Figure 19. Effect of BAM on Subjective Ratings (at each of the four seat positions) at constant speeds



Engine RPM	Subjective Rating (Driver's Ear)			
	Without BAM	Sound Quality	With BAM	Sound Quality
1500	5.5	Boom / Modulation	9	Good
2000	5.5	Light Boom / Mod	7	Light Mod / Grinding
2500	4.5	Low Freq Modulation	5.5	Modulation / Rough

Figure 20. Effect on Driver's Ear of Intake & Exhaust BAM treatment during various steady state operating conditions

#### 5.1.2. Equal Length Y-Pipe

On the GMC Yukon Denali the exhaust system consists of a single exhaust pipe layout from the third catalyst/ flex-joint backward. The system is mounted on the right side of the vehicle from the chassis frame and therefore the downpipes are of unequal length. For DSF mode this causes unpleasant acoustics, as describe is section 2 and 3. If equal length downpipes can be incorporated (see Figure 21) early on in the vehicle development program then the acoustic sound quality can be improved significantly (less roughness, muddiness, etc.)



Figure 21. Equal Length versus Standard Y-pipe

The Tailpipe sound data is shown below in Figure 22, showing the effectiveness of the equal length system in reducing the sidebands that cause the fluctuation of the *fire-skip-skip* pattern.

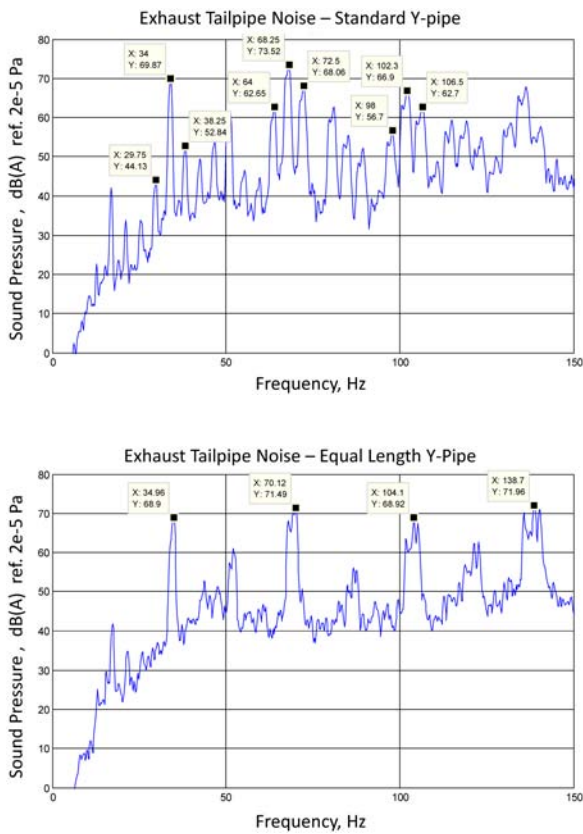


Figure 22. Averaged Tailpipe Noise for Standard (top) versus Equal Length (bottom) Y-pipe systems using the fire-skip-skip pattern

Notice the substantial reduction in the sidebands, indicating a corresponding reduction in the fluctuation of the tailpipe noise. (Note that the broadening of the lobes at higher frequency is an artifact of uneven RPM control during data collection)

### 5.1.3. Exhaust Control Valve

Many vehicles have already made use of ECV's for reducing low frequency noise instead of using larger muffler volumes. When used with DSF the results are very impressive, reducing the low frequency and pulsation / modulation issues that cause poor in-cabin noise issues.

A typical ECV valve is shown in Figure 23.



Figure 23. Prototype Exhaust Control Valve [13] with passive spring operation

Figure 24 shows the effectiveness of the ECV in controlling low frequency noise in the exhaust system. Note the reduced order content and reduction in the resonance mode

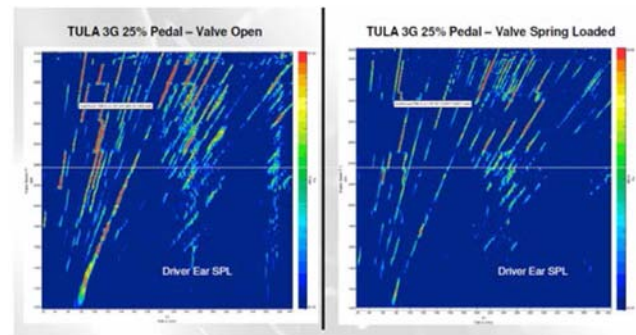


Figure 24. Effectiveness of the ECV at reducing interior cabin noise

### 5.1.4. Active Noise Control

Currently the production Yukon Denali vehicle uses an Active Noise Control system that utilizes a sub-woofer to address the boom (cabin resonant frequency) and other low frequency content. As seen in Figure 17, different firing patterns can alter the acoustic spectrum from the standard V8 sound, and also have much lower frequencies. Using ANC with DSF is an ongoing area of investigation.

## 5.2. Vibration Mitigation

Vibration due to DSF can be roughly described as one of two different types. The first type, described in Section 1 arises through the forces from the engine driving the vehicle, causing fore-aft vehicle acceleration. The second type of vibration arising from DSF is from the motion of the engine or other powertrain components.

In addition to abilities in the software to minimize excitation, there are a number of methods that have been used in previous cylinder de-activation vehicles that can help mitigate the vibration arising from both types of vibration

### 5.2.1. Torque Converter Clutch Slip

Vehicles fitted with an automatic transmission have the ability to slip the torque converter to minimize the variation in torque, through damping and friction. However, higher slip reduces fuel economy so there has to be an optimization of the slip with NVH. This is an example of mitigating the first type of vibration.

### 5.2.2. Active Engine & Transmission Mounts

For mitigation of the second type of vibration, consider the engine mounts. The 2010 Yukon has limited isolation across the Transmission Mount in the 30 Hz to 100 Hz range, regardless of engine operating condition. See Figure 25. The black lines show measurements on the active side of the mount, while the blue lines show measurements on the passive side.

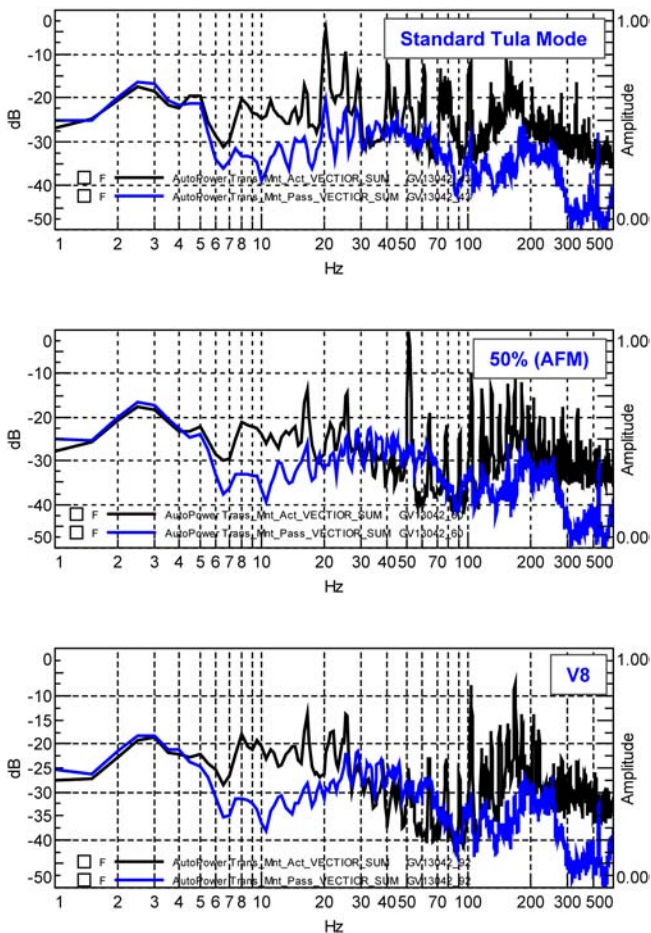


Figure 25. Isolation across the mounts, 10dB considered a minimum requirement across the frequency range (25 Hz to 100 Hz poor in this example)

Active mounts can significantly improve isolation at higher frequencies (30 Hz to 200 Hz) [13] as well as provide powertrain rigid body control below 30 Hz. Due to their high speed control, active mounts can provide a lot of synergy with DSF technology.

### 5.2.3. Other Transfer Paths & Modal Sensitivities

As mentioned previously, the identification and treatment of low frequency transfer paths is important when running DSF. Some paths currently being investigated at Tula are

- Powertrain Mount / Sub-frame Mount Sensitivity
- Exhaust Hanger Isolator / Sensitivity
- Steering Wheel / Column Sensitivity

## SUMMARY/CONCLUSIONS

The DSF system incorporating any-time, any-cylinder deactivation offers impressive fuel economy benefits. This paper has discussed ways of obtaining the benefits without compromising the driving experience. Near-production NVH levels are achieved, either without vehicle modification or using well understood physical mitigation techniques.

Simple theoretical models have been given to predict the effect of a chosen pattern on both vibration and acoustics. These allow an intuitive understanding of the effect of DSF, and can also predict which patterns will create unacceptable noise or vibration issues. A prime example was the acoustic fluctuation produced by the *fire-skip-skip* pattern when used with unequal length Y-pipes. These models also provide insight into the tradeoffs of algorithm-only mitigation of the noise and vibration issues.

To further enable tuning for noise and vibration, objective metrics have been presented that correlate to subjective sensations. Sperling's method has been mapped to a common 1-10 Subjective scale, and a method of computing the amount of acoustic fluctuation has also been derived.

Finally, a number of physical mitigation methods have been presented. When initial evaluations of the *fire-skip-skip* pattern revealed an intense acoustic fluctuation, an exhaust BAM isolated this noise to the tailpipe emission. After analysis of the problem revealed the effect of the unequal-length Y-pipe, modifications of the exhaust system verified that this was the source. Further development showed that an ECV provided excellent mitigation of the problem for lower cost. Likewise, controlled slip of the TCC was used as a mitigating technique to reduce vibration into the cabin. Other NVH enablers are available and are being investigated in collaboration with Tula's customers.

The techniques presented: algorithmic, system design, and physical mitigation all show effectiveness in maintaining NVH quality to permit realization of significant fuel efficiency gains provided by DSF engine operation.

## REFERENCES

1. Wilcutts, M., Switkes, J., Shost, M., and Tripathi, A., "Design and Benefits of Dynamic Skip Fire Strategies for Cylinder Deactivated Engines," *SAE Int. J. Engines* 6(1):278-288, 2013, doi:[10.4271/2013-01-0359](https://doi.org/10.4271/2013-01-0359).
2. Stabinsky, M., Albertson, W., Tuttle, J., Kehr, D. et al., "Active Fuel Management™ Technology: Hardware Development on a 2007 GM 3.9L V-6 OHV SI Engine," SAE Technical Paper [2007-01-1292](https://doi.org/10.4271/2007-01-1292), 2007, doi:[10.4271/2007-01-1292](https://doi.org/10.4271/2007-01-1292).
3. Falkowski, A., McElwee, M., and Bonne, M., "Design and Development of the DaimlerChrysler 5.7L HEMI® Engine Multi-Displacement Cylinder Deactivation System," SAE Technical Paper [2004-01-2106](https://doi.org/10.4271/2004-01-2106), 2004, doi:[10.4271/2004-01-2106](https://doi.org/10.4271/2004-01-2106).
4. Fujiwara, M., Kumagai, K., Segawa, M., Sato, R. et al., "Development of a 6-Cylinder Gasoline Engine with New Variable Cylinder Management Technology," SAE Technical Paper [2008-01-0610](https://doi.org/10.4271/2008-01-0610), 2008, doi:[10.4271/2008-01-0610](https://doi.org/10.4271/2008-01-0610).
5. Suzuki, N., Hayashi, Y., Odell, M., Esaki, T. et al., "Development of New V6 3.5L Gasoline Engine for ACURA RLX," *SAE Int. J. Engines* 6(1):629-636, 2013, doi:[10.4271/2013-01-1728](https://doi.org/10.4271/2013-01-1728).
6. Peras, L., "Internal Combustion Engines", U.S. Patent 2771867, 1956.
7. Förster, H.J., Lübbling, B.E., Letsche U., "Process and Apparatus for Intermittent Control of a Cyclically Operating Internal Combustion Engine", U.S. Patent 4509488, 1982.
8. ISO-2631-1:1997(E), Mechanical vibration and shock - Evaluation of human exposure to whole-body vibration, 1997.
9. Mansfield, N., "Literature Review on Low Frequency Vibration Comfort", Report under EC- Asia Link Program, ASIE/ 2005/ 111000, 2006.
10. Sperling, E. and Betzhold, C., "Beitrag zur Beurteilung des Fahrkomforts in Scheinenfahrzeugen", *Glaser's Annalen*, 80, pp 314-320, 1956.
11. Kim, Y., Kwon, H., Kim, S., Park C., and Park, T., "Correlation of ride comfort evaluation methods for railway vehicles", *Proceedings of the Institution of Mechanical Engineers Part F - Journal of Rail and Rapid Transit*, 217(2), pp. 73-88, 2003.
12. Narayanamoorthy, R., Saran, V.H., Goel, V.K., Harsha, S.P., et al, "Determination of Activity Comfort in Swedish Passenger Trains", 8<sup>th</sup> World Congress on Railway Research (WCRR 2008), May 18-22, 2008, COEX, Seoul, Korea.
13. Zwicker E, and Fastl, H., *Psychoacoustics. Facts and Models* 3<sup>rd</sup> edition (Springer, Heidelberg, New York, 2007).
14. ANSI S1.4-1983, American National Standard - Specification for Sound Level Meters, 1983.
15. Faurecia Adaptive Valve(tm) is the intellectual property of Faurecia Emissions Control Technologies
16. Swanson, D., "Active Engine Mounts for Vehicles," SAE Technical Paper [932432](https://doi.org/10.4271/932432), 1993, doi:[10.4271/932432](https://doi.org/10.4271/932432).

## CONTACT INFORMATION

Joe Serrano:

[joe@tulatech.com](mailto:joe@tulatech.com)

## ACKNOWLEDGMENTS

Thanks to the following Tula Team for supporting this paper:

Steve Carlson, Chris Chandler, Mark Wilcutts, Xin Yuan, Adya Tripathi

## DEFINITIONS/ABBREVIATIONS

**CAFE** - Corporate Average Fuel Economy

**DSF** - Dynamic Skip Fire

**OEM** - Original Equipment Manufacturer

**MAP** - Manifold Air Pressure

**BAM** - Big Auxiliary Muffler

**TCC** - Torque Converter Clutch

**GM** - General Motors

**SUV** - Sports Utility Vehicle

**ISO** - International Standards Organization

**LMS** - Leuven Measurement Systems

**RPM** - Revolutions Per Minute

**ECV** - Exhaust Control Valve

**ANC** - Active Noise Control